



## ORIGINAL ARTICLE

# Morphology, behavior, and phylogenomics of *Oxytoxum lohmannii*, Dinoflagellata

Elizabeth C. Cooney<sup>1</sup>  | Dean M. Jacobson<sup>2</sup> | Gordon V. Wolfe<sup>3</sup> | Kelley J. Bright<sup>4</sup> | Juan F. Saldarriaga<sup>1</sup> | Patrick J. Keeling<sup>1</sup> | Brian S. Leander<sup>1,5</sup>  | Suzanne L. Strom<sup>4</sup>

<sup>1</sup>Department of Botany, University of British Columbia, Vancouver, British Columbia, Canada

<sup>2</sup>College of the Marshall Islands, Majuro, Marshall Islands

<sup>3</sup>Department of Biological Sciences, California State University, Chico, Chico, California, USA

<sup>4</sup>Shannon Point Marine Center, Western Washington University, Anacortes, USA

<sup>5</sup>Department of Zoology, University of British Columbia, Vancouver, British Columbia, Canada

## Correspondence

Elizabeth C. Cooney, Department of Botany, University of British Columbia, Vancouver, BC, Canada.

Email: [lizcooney22@gmail.com](mailto:lizcooney22@gmail.com)

## Funding information

Natural Sciences and Engineering Research Council of Canada, Grant/Award Number: NSERC 2019-03986 and NSERC 2019-03994; National Science Foundation, Grant/Award Number: OCE-9730952; Gordon and Betty Moore Foundation, Grant/Award Number: <https://doi.org/10.37807/GBMF9201>

## Abstract

Dinoflagellates are an abundant and diverse group of protists representing a wealth of unique biology and ecology. While many dinoflagellates are photosynthetic or mixotrophic, many taxa are heterotrophs, often with complex feeding strategies. Compared to their photosynthetic counterparts, heterotrophic dinoflagellates remain understudied, as they are difficult to culture. One exception, a long-cultured isolate originally classified as *Amphidinium* but recently reclassified as *Oxytoxum*, has been the subject of a number of feeding, growth, and chemosensory studies. This lineage was recently determined to be closely related to *Prorocentrum* using phylogenetics of ribosomal RNA gene sequences, but the exact nature of this relationship remains unresolved. Using transcriptomes sequenced from culture and three single cells from the environment, we produce a robust phylogeny of 242 genes, revealing *Oxytoxum* is likely sister to the *Prorocentrum* clade, rather than nested within it. Molecular investigations uncover evidence of a reduced, nonphotosynthetic plastid and proteorhodopsin, a photoactive proton pump acquired horizontally from bacteria. We describe the ultrastructure of *O. lohmannii*, including densely packed trichocysts, and a new type of mucocyst. We observe that *O. lohmannii* feeds preferentially on cryptophytes using myzocytosis, but can also feed on various phytoflagellates using conventional phagocytosis. *O. lohmannii* is amenable to culture, providing an opportunity to better study heterotrophic dinoflagellate biology and feeding ecology.

## KEY WORDS

dinoflagellate, grazing, nonphotosynthetic plastid, peduncle feeding, phylogenomics, proteorhodopsin

## INTRODUCTION

DINOFLLAGELLATES are a diverse group of protists that account for a significant percentage of the eukaryotic plankton in the ocean (Keeling & del Campo, 2017; Taylor et al., 2008). These alveolates play a wide range of ecological roles due, in part, to their range of trophic strategies, including widespread mixotrophy among photosynthetic taxa

(Stoecker, 1999) as well as strict heterotrophy. These trophic states are polyphyletic, as both plastid acquisition and reduction have occurred multiple times independently over the evolutionary history of the group (Cooney et al., 2024; Hehenberger et al., 2014; Janouškovec et al., 2017; Keeling, 2013; Saldarriaga et al., 2001; Sarai et al., 2020).

Heterotrophic dinoflagellates include free-living, parasitic, and mutualist symbiont taxa (Gaines &

This contribution is dedicated to the memory of Dean M. Jacobson, who passed away December 27, 2018.

This is an open access article under the terms of the [Creative Commons Attribution-NonCommercial-NoDerivs](https://creativecommons.org/licenses/by-nc-nd/4.0/) License, which permits use and distribution in any medium, provided the original work is properly cited, the use is non-commercial and no modifications or adaptations are made.

© 2024 The Author(s). *Journal of Eukaryotic Microbiology* published by Wiley Periodicals LLC on behalf of International Society of Protistologists.

Elbrächter, 1987; Schnepf & Elbrächter, 1992). Free-living heterotrophs are major consumers in marine systems (Jeong et al., 1999; Sherr & Sherr, 1994) and display a wide range of nutritional strategies and specializations, including phagocytosis, myzocytosis (feeding via perforation of prey cell), and pallium feeding (Hansen & Calado, 1999; Jacobson & Anderson, 1986). The diversity of chemosensory abilities and feeding specificities of heterotrophic dinoflagellates is likely equally broad (Hansen & Calado, 1999; Jacobson & Anderson, 1986; Levandowsky & Hauser, 1975). Parasitic and symbiotic taxa use chemosensory cues to locate hosts (Fitt, 1985; Schnepf & Drebes, 1986), while free-living taxa display a wide range of chemosensory feeding abilities. Some, like *Oxyrrhis marina*, can respond chemotactically (Fenchel, 2001; Spero, 1985), but are indiscriminate tactile feeders that phagocytose inert material and almost all potential prey (Hansen, 1992; Strom, Wolfe, Holmes, et al., 2003; Strom, Wolfe, Slajer, et al., 2003). *Cryptocodinium cohnii* is another indiscriminate feeder that responds to nanomolar levels of chemical cues in the environment (Hauser, Levandowsky, & Glassgold, 1975; Hauser, Levandowsky, Hutner, et al., 1975). In contrast, many taxa are highly specialized feeders and use chemosensory cues to locate specific prey (Jacobson & Anderson, 1986, 1992; Larsen, 1988).

Compared to their photosynthetic counterparts, heterotrophic dinoflagellates are generally under-sampled and understudied in phylogenomic analyses, due to the difficulty of cultivating these lineages. However, the ecological importance and biological diversity of these groups demonstrate the need for further study. One taxon, recently classified as *Oxytoxum lohmannii* (previously *Amphidinium longum*), has appeared periodically in the literature since its first description over a century ago (Kofoid & Swezy, 1921; Wilcox & Wedemayer, 1991). It has been used in several studies of planktonic protist chemical sensing and defense (Strom et al., 2018; Strom, Wolfe, Holmes, et al., 2003; Strom, Wolfe, Slajer, et al., 2003), but its phylogenetic placement has so far only been explored using ribosomal DNA sequences (Gottschling et al., 2024; Saldarriaga et al., 2001) and has yet to be resolved. Here, using phylogenomic analysis, we build on recent findings that this taxon represents a distinct heterotrophic lineage related to the largely photosynthetic *Prorocentrum* clade, and show genetic evidence for a remnant nonphotosynthetic plastid and a possible alternative phototrophic mechanism, proteorhodopsin. We describe the cell biology of this dinoflagellate in the context of its ecology, including ultrastructure, growth potential, and swimming and feeding behavior.

## MATERIALS AND METHODS

### Maintenance cultures

Cells identified at the time of collection in 1993 as *Amphidinium longum* (now called *Oxytoxum lohmannii*; Gottschling et al., 2024) were isolated from the Salish Sea

near Anacortes, WA (48°30.6' N, 122°40.2' W), and maintained in culture for many years, contributing to multiple studies (Chu et al., 2009; Nielsen & Kjørboe, 2015; Saldarriaga et al., 2001; Strom et al., 2018; Strom & Morello, 1998; Strom, Wolfe, Holmes, et al., 2003; Strom, Wolfe, Slajer, et al., 2003). Cultures were grown in filtered, autoclaved coastal seawater (salinity=30, temperature=13–15°C) enriched with low concentrations of trace metals and fed weekly on a mixed diet of *Isochrysis galbana* (haptophyte), *Rhodomonas salina* (cryptophyte), and *Emiliania huxleyi* (haptophyte). Cultures were transferred every 2 weeks. Growth, feeding, and swimming observations were usually conducted at 13–15°C or room temperature. The original isolate (SPMC98) was lost in 2004 after its use in the imaging portions of this study. Another morphologically indistinguishable isolate (SPMC100) collected from the same location was established in 2003 and the resulting culture was used to generate molecular data in the present study. Feeding observations have been reported from both SPMC98 (Strom & Loukos, 1998; Strom & Morello, 1998) and SPMC100 (Strom et al., 2020). Assessment of growth on different cryptophyte species and isolates used the method described in Strom and Morello (1998).

### Epifluorescence microscopy

Predator and prey subsamples were preserved in glutaraldehyde (final conc. 0.5%), stained with DAPI, and filtered onto 25-mm, 1.0- $\mu$ m pore-size polycarbonate filters (Poretics). Filters were mounted in low-fluorescence immersion oil on microscope slides and examined with a Leica DM microscope under UV excitation (DAPI nuclear staining) or blue excitation (ingested prey chloroplast autofluorescence) and photographed with a 35-mm camera. Lectin staining of trichocysts (Concanavalin A; ConA) was performed as described in Strom, Wolfe, Holmes, et al. (2003).

### SEM

Cells were fixed with 4% isotonic osmium tetroxide to 0.2% final concentration. Fixation with 1%–2% electron microscopy grade glutaraldehyde caused cell distortion, loss of flagella, and trichocyst discharge. Fixed cells were filtered by gravity or vacuum (<5 mm Hg) onto 13-mm polyester filters (Poretics; 1–3- $\mu$ m pores). Filters were rinsed with distilled water and dehydrated in an ethanol series (50%, 70%, 100%), critical-point dried with CO<sub>2</sub> to 50 bar/40°C with a Balzers Union CPD 020, and finally vacuum evaporation-coated with 60/40 Au/Pd. Specimens were viewed on a Hitachi S-430 SEM at 10 kV and digitized with 'Printerface' (GW Electronics).

## TEM

Cells were concentrated by gentle centrifugation and fixed in a final concentration of 2% glutaraldehyde buffered with 0.1-M cacodylate. After 1 h of fixation, cells were pipetted onto a thin slab of agarose on a plastic microscope slide. Using a compound microscope, groups of approximately 12 cells were pushed (using a loop of finely drawn-out capillary tube glass, functioning like a shepherd's crook) close together. In this way all cells had a similar orientation (i.e., their longitudinal axis was restricted to a common plane), facilitating comparisons among cells. The cells were then enrobed beneath a top layer of agarose, taking extreme care not to disturb the cell arrangement. The agar containing the cells was cut into a 1- to 2-mm block, rinsed in buffer, and postfixed in 1% osmium tetroxide. To allow the cell cluster to be detected using a dissecting scope (given that *O. lohmannii* does not blacken significantly during osmication), a larger dinoflagellate obtained from a net tow of Puget Sound (e.g., *Scrippsiella* or *Dinophysis*) was included in the cell cluster. Agar blocks were then rinsed in dH<sub>2</sub>O, dehydrated in an acetone series, and Epon-embedded using Epon-acetone mixtures containing progressively higher proportions of Epon. After polymerization in a clear silicone rubber embedding mold, thin sections were made on a LKB ultramicrotome and collected on Pioloform-coated 1 × 2-mm slot grids, which were conventionally stained with lead citrate and uranyl acetate and examined on a Hitachi H-300 transmission electron microscope.

## Single-cell sequencing and transcriptome assembly

Individual cells were isolated from cultures to avoid including prey in transcriptome sequencing. Cells were picked under a Leica DMIL inverted light microscope using modified Pasteur pipettes and washed in filter sterilized water from the same culture (0.2- $\mu$ m filter). Isolated cells were placed in lysis buffer, grouping 4–6 cells to a tube. cDNA was generated, amplified, and cleaned according to the Smart-seq2 protocol (Kolisko et al., 2014; Picelli et al., 2014), and Illumina libraries were prepared (Nextera Flex) and sequenced on the Miseq platform at the Sequencing and Bioinformatics Consortium at University of British Columbia (raw reads available in the Sequence Read Archive under project PRJNA1063374). Raw reads for all samples were combined and trimmed with Cutadapt (Martin, 2011), specifying Nextera adapters and Illumina-specific primers for removal. Transcriptome assembly was performed with rnaSPAdes v3.13.2 (Bankevich et al., 2012) and contaminants were identified and removed using megaBLAST to search against Uniprot reference proteomes for divergent contigs. Blobplots was used to visualize contigs by taxonomic assignment, and unwanted taxonomic categories associated with prey and bacteria were removed. Open reading frames were identified using TransDecoder

v5.1.0 (Haas et al., 2013) and annotation was performed using BlastP (Altschul et al., 1990) against the SwissProt database (Poux et al., 2017) with an e-value threshold  $1e10^{-5}$ .

Three individual cells were also picked from environmental samples collected from Jericho Pier in Vancouver, BC, two on July 14 (cells A and B) and one on October 2, 2020 (cell C). Each cell was video recorded (see <https://doi.org/10.5281/zenodo.11458711>), washed, and isolated in lysis buffer separately. These samples were then treated identically to culture samples in all other downstream processes and analyses.

## Phylogenomic analysis

Predicted peptide transcriptomes were searched with BlastP, using curated protein alignments of 263 genes as queries (Burki et al., 2016). Hits were aligned with their respective queries and IQ-TREE v1.6.12 was used to generate maximum likelihood (ML) trees (model: LG+G; Stamatakis, 2006). Removal of paralogs, isoforms, and contaminants was performed after visual inspection of each tree to identify unwanted sequences. Cleaned alignments were selected and processed using SCaFoS v4.55 (Roure et al., 2007), limiting the data set to include only genes present in at least 60% of the relevant operational taxonomic units (242 genes total). IQ-TREE was used to generate a final ML tree from the concatenated alignment using 1000 ultrafast bootstraps (–bb 1000; Hoang et al., 2018) and the empirical profile mixture model LG+C60+F+G4 (Quang et al., 2008). A second tree was generated for comparison, using 100 bootstraps (–b 100) and LG+C60+F+G4 PMSF, with the previous ML tree as the guide tree (Wang et al., 2018).

A BlastN search for small subunit ribosomal RNA gene sequences (SSU rDNA) was conducted on assembled transcriptome data using the SSU rDNA of *Prorocentrum micans* (accession number AY833514.1) as a query. Hits were added to a manually curated alignment of dinoflagellate SSU rDNA, aligned with MAFFT v7.475 (Kato & Standley, 2013), and trimmed with trimAl v3 (80% gap threshold) (Capella-Gutiérrez et al., 2009). ML tree construction was performed using ultrafast bootstrap approximation (–bb 1000) and ModelFinder (Kalyaanamoorthy et al., 2017) to determine the best fit model (GTR+F+I+G4) in IQ-TREE. SSU rDNA sequences for both cultured and wild cells are available in GenBank under the accession numbers PP110230–PP110233.

## Organelle and photoactivity-associated protein characterization

All transcriptomes were searched for rhodopsins, retinal biosynthesis enzymes, and plastid-associated enzymes involved in the biosynthesis of heme, isoprenoid,



and iron–sulfur clusters. BlastP searches were performed using dinoflagellate homologs as queries and an *e*-value threshold of  $1e^{-25}$ . To filter out contaminants and confirm that the resulting hits belonged to the host cells, these sequences were aligned with curated collections of corresponding diverse eukaryote and prokaryote homologs (Hehenberger et al., 2019). These alignments were then trimmed with an 80% gap threshold in trimAl and analyzed with IQ-TREE using  $-bb$  1000 and ModelFinder to infer ML trees for each enzyme. In the untrimmed alignments, each sequence was visually inspected for an N-terminal extension through comparison with bacterial homologs, which lack signal and transit peptides. For sequences possessing an N-terminal extension, SignalP v3.0 (for cleavage site visualization) and v5.0 were used to predict the presence of signal peptides (Nielsen et al., 1997), and transmembrane regions were predicted using TMHMM v2.0 (Sonnhammer et al., 1998).

## RESULTS

### General description and cytology

The *O. lohmannii* cells used in this study are approximately 22 by 16  $\mu\text{m}$  in size and ellipsoidal in shape, although cell size and shape are known to vary substantially between starved and well-fed cells (Gottschling et al., 2024; Strom & Morello, 1998). Cells have a pronounced episome and a single, large, centrally located food vacuole approximately 5–6  $\mu\text{m}$  in diameter (Figure 1A; Figure S1A,B). Transverse and longitudinal flagella are inserted close to the base of the anteriorly directed peduncle (Figure 1B), situated at the base of the episome along the ventral side, just above the sulcus. The peduncle has a slender keel or tongue-like form, with the distal 5  $\mu\text{m}$  protruding from the ventral epitheca (Figure 1B–D; Figure S1A–C). A regular arrangement of lateral trichocyst pores occurs on all hypothecal plates, typically involving three or four vertical columns and seven or eight horizontal rows (Figure 1B–D). Each trichocyst column occupies a continuous raised longitudinal surface ridge (Figure S1D). A row of pores, situated immediately below the cingulum, is spaced more than twice as closely as the trichocyst pores located to the posterior (Figure 1C).

### Ultrastructure

*Oxytoxum lohmannii* ultrastructure is conventional, including typical trichocysts and a standard dinoflagellate nucleus with electron dense chromosomes and nucleolus (Figure 2). Each cell has nearly 200 trichocysts, an unusually high number for a cell of this size. The pattern of

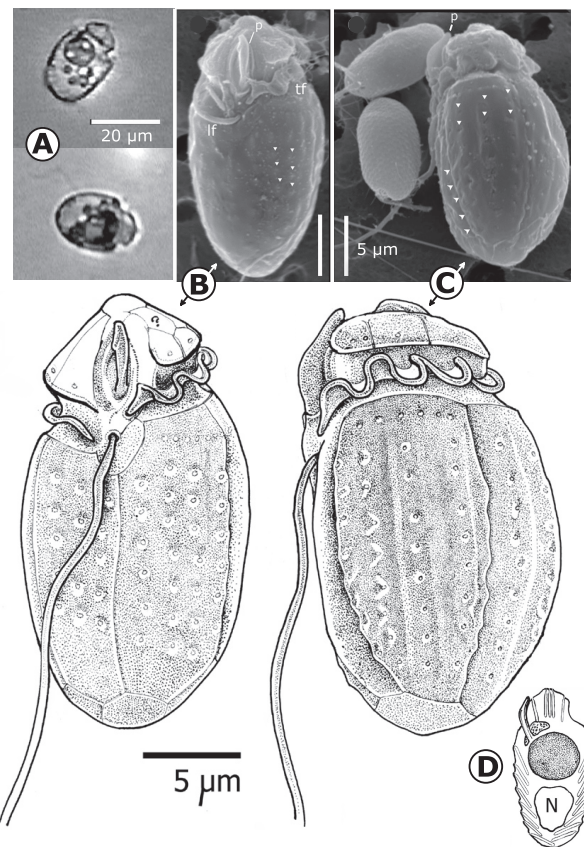


**FIGURE 1** Microscopic images and depictions of *Oxytoxum lohmannii* (SPMC98). (A) Brightfield images of live *O. lohmannii* cells. Note conspicuous central food vacuole. Bottom image shows longitudinal flagella protruding at top of cell. (B) SEM and illustrated depiction of a ventral view of *O. lohmannii* showing peduncle (p) and the longitudinal and transverse flagellum (lf, tf). Trichocyst pores are indicated by arrowheads. Illustration shows the likely arrangement of *O. lohmannii* thecal plates. Scale bar = 5  $\mu\text{m}$ . (C) SEM and illustrated depiction of cell's left lateral side, showing peduncle (p) in contact with cryptophyte prey. Note regular rows and columns of trichocyst pores (arrowheads). (D) Diagrammatic longitudinal section showing orderly trichocyst arrangement, and peduncle and food vacuole.

trichocyst distribution is striking; those situated in the apical region are parallel with the cell's longitudinal axis and regularly spaced (Figures 1D and 2A). Trichocysts in the episome, which are angled outward approximately 30 degrees from this axis, are also regularly arranged in tiers; external trichocyst pores, visible with SEM, are arrayed in regularly spaced rows and columns (Figures 1B–D and 2B).

A previously unknown type of mucocyst-like vesicle is present (with variable abundance) in all cells (Figure 2C,B; Figure S1A). Most mucocyst vesicles are ellipsoid and contain two components: fibrillar material (similar to the contents of some dinoflagellate mucocysts) and several central profiles of electron dense granular material. The latter seems to be a single elongate structure that is often coiled in a helical configuration. No other extrusomes are present.

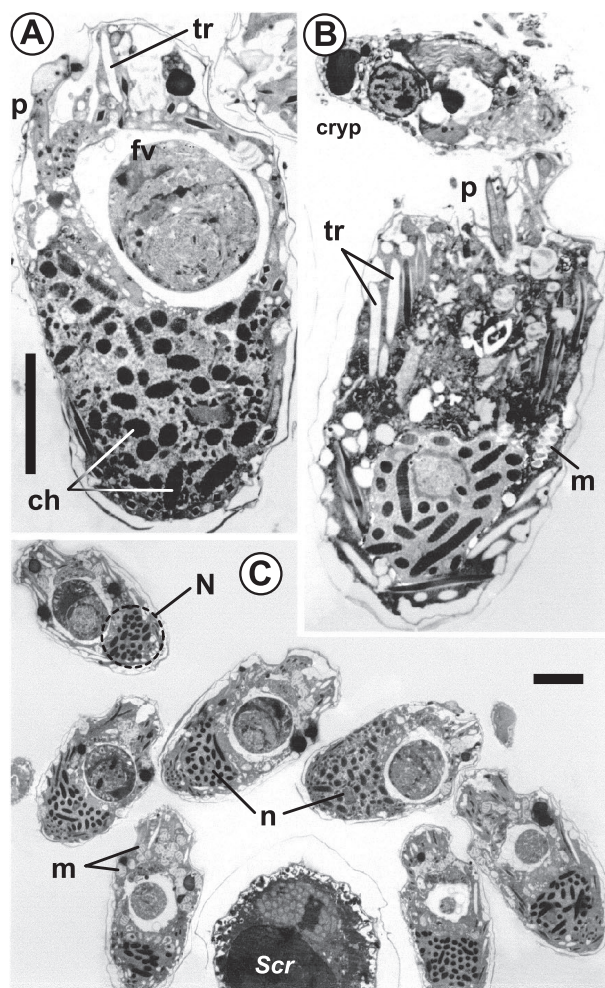


**FIGURE 2** TEMs showing whole cell ultrastructure of *Oxytoxum lohmannii* (SPMC98). (A) Longitudinal whole cell section, containing a two-sectioned food vacuole (fv) and an emergent peduncle (p). Also visible are an apical trichocyst (tr) and condensed chromosomes (ch). (B) Longitudinal whole cell section, showing peduncle juxtaposed to a cryptophyte prey cell (cryp), in the position typical of the feeding configuration. Note parallel, uniformly arranged trichocysts (tr) and mucocyst (m). (C) Hand-manipulated cluster of seven longitudinal whole cell profiles showing consistency of nuclei (N), nucleoli (n) food vacuole position, etc. All cells contain novel mucocysts (m) at varying abundances. *Scrippsiella* sp. cell (*Scr*) added for enhanced visibility of cell cluster embedded within plastic block. Scale bars = 5 μm (bar in panel A also applies to B).

## Flagellar apparatus

The longitudinal flagellum is shown within the flagellar pore in [Figure S1E](#), and the microtubules of the longitudinal flagellar root are visible in [Figure S1F](#). A partial reconstruction is shown in [Figure S1](#) as having 17 microtubules. This root lies directly below the cell cortex. The striated collar of the transverse flagellum appears to form an attachment with the nearby surface of the thecal wall that forms the flagellar pore of the longitudinal flagellum ([Figure S2A,G](#)). Collared pits appear on both the flagellar canal of the

longitudinal flagellum and the transverse flagellum ([Figure S2C,G,I](#)). The basal bodies appear to lie at an approximate right angle with respect to each other ([Figure S2C,F,I,L](#)).

## Peduncle structure

The peduncle has two structural components. The first is an elongate tube, the distal end of which is visible on the exterior of the cell, anterior to the cingulum, resting within a furrow running from the basal body region on the cell's ventral surface toward the cell apex ([Figure 1B](#), [Figure S1A–D](#)). The second is a larger internal region adjacent to the central food vacuole ([Figure S1E](#)). Both regions contain a characteristic mix of electron dense bodies and electron lucent vacuoles, most containing one to several internal membrane profiles, but the interior region has the highest density of electron dense vesicles. These vesicles are typical of those found adjacent to the microtubular ribbon or basket in a diverse assemblage of dinoflagellates. The anterior-most end of the peduncle often has a pointed shape, reminiscent of a narrow arrowhead ([Figure 1B](#), [Figure S1B,C](#)) and features large regions of either vacuolar space, containing a uniform, flocculant material or empty, convoluted vacuolar profiles that resemble dilated endoplasmic reticulum ([Figure S1A–F](#), [Figure S2A–F](#)). The peduncle lacks a striated collar, and while the two regions of the peduncle appear separate in many cross sections, they are clearly continuous. A distinct peduncular population of microtubules, each 18–20 nm in diameter, are visible at the outer edge ([Figure S1F](#) lower inset).

## Food vacuole structure

The elongate shape and small size of this species constrains the location of the food vacuole to a central position, anterior to the nucleus ([Figure 1A](#)). Often a food vacuole is composed of two or more distinct internal regions, appearing as a sphere embedded (off center) within the larger sphere of the food vacuole ([Figure 2A](#), [Figure S1A,B](#)). This is perhaps the result of either multiple feeding episodes, an interruption during one meal, or differences in the viscosity of ingested cytoplasm and organelles.

## Phylogenomic analysis

The transcriptome assembly for cultured *O. lohmannii* had the most predicted peptides of all the transcriptomes and was the most complete, according to BUSCO v5 coverage estimates and the presence of genes within the multigene analysis ([Figure S3](#)). In comparison, assemblies for the wild single cells A and B had less than half the



number of predicted peptides but were only marginally less complete than that of the culture. Cell C had the fewest peptides and very low coverage compared to all other transcriptomes, likely due to mRNA degradation at the time of sampling.

A maximum likelihood analysis of 242 genes placed *O. lohmannii* as branching sister to the genus *Prorocentrum* with full node support (Figure 3). Transcriptomes from single cells collected from environmental samples grouped with the *O. lohmannii* culture, and a second PMSF analysis confirmed these relationships, with a bootstrap score of 100 for the relationship of *O. lohmannii* with *Prorocentrum* (Figure 3). SSU rDNA sequences for all cells and culture were identical to one another, although sequences for cells A and C were truncated (Figure S4).

### Plastid and rhodopsin-related proteins

Proteins from the plastid-derived biosynthesis pathways for heme, isoprenoids, and iron–sulfur clusters were found in all transcriptomes except for cell C (Figure 4, Data S1). No transcriptome had complete coverage of any single pathway, but the combination of transcripts recovered from all three transcriptomes accounted for all but eight of the 24 expected enzymes (Figure 4). Most recovered sequences were truncated, missing the N-terminus of the active protein as well as any indication of an N-terminal extension. Transcripts for *sufE*, *hemL*, and *hemF* had N-terminal extensions with predicted signal peptides and transmembrane regions, while *sufB*, *petF*, and *hemC* had unidentified extensions that lacked bipartite signal characteristics.

In phylogenies constructed for each enzyme (<https://doi.org/10.5061/dryad.9zw3r22pp>), *O. lohmannii* transcripts clustered within the clade of homologs from peridinin-type plastids. The only exception to this was *sufD*, for which transcripts from the *O. lohmannii* culture and cell A branched outside of and sister to all other peridinin-type plastid-derived homologs. In addition to a peridinin-type homolog for *hemE* from the culture transcriptome, a homolog from cell B grouped within a separate dinoflagellate clade sister to haptophytes. Likewise, *sufS* from the culture sample fell within the clade of peridinin-type plastid homologs while a transcript from cell A clustered with apicomplexans, suggesting the latter was a possible contaminant sequence. Contaminant homologs of *sufB*, *petF*, *hemA*, and *hemL* were picked up from cell A, possibly the result of recent prey consumption. In the case of *petF*, the presumed contaminant clustered within *Symbiodinium* and the possibility that it was the result of a recent gene duplication could not be eliminated.

A search for rhodopsins recovered hits from all four transcriptomes. When placed into a phylogeny of rhodopsins, *O. lohmannii* transcripts clustered with

dinoflagellate (including *Prorocentrum*) proteorhodopsins sister to stramenopiles (Figure S5A). Rhodopsin transcripts from the culture transcriptome were similar to but phylogenetically distinct from those of the three wild cells. All functional residues previously described in *Oxyrrhis marina* proteorhodopsin were conserved in *O. lohmannii*, with the exception of a Ser replacing a Gly on the first helix in the retinal binding pocket (Figure S5B; Slamovits et al., 2011). Like *O. marina*, *O. lohmannii* peptide sequences contained a leucine residue in the third helix, indicative of green light activation (Man et al., 2003).

The enzymes *crtB*, *crtI*, and *crtY* that make up the carotenoid biosynthesis pathway were absent from all *O. lohmannii* transcriptomes. However, homologs from the carotenoid cleavage oxygenase (CCO) family of enzymes were present in all samples except cell C. Using InterProScan (Blum et al., 2021) truncated transcripts were identified as belonging to three different but closely related functional orthologs:  $\beta,\beta$ -carotene 15,15'-dioxygenase, carotenoid 9,10(9',10')-cleavage dioxygenase 1, and a putative apocarotenoid dioxygenase. In a collective phylogeny of these proteins (<https://doi.org/10.5061/dryad.9zw3r22pp>), transcripts from different samples within each ortholog were generally disparate, with the exception of carotenoid 9,10(9',10')-cleavage dioxygenase 1, for which transcripts of cells A and B were identical.

### Nutrition and feeding behavior

*Oxytoxum lohmannii* can be maintained indefinitely in culture, growing at rates of 0.1–0.5 day<sup>-1</sup> (see Discussion) up to maximum observed densities of ca. 3500 mL<sup>-1</sup>. We found that *O. lohmannii* will feed and grow on a range of microalgal prey, including coccolithophorids (*Emiliania huxleyi*), prymnesiophytes (*Isochrysis galbana*), prasinophytes (*Mantoniella squamata*) and small dinoflagellates (*Heterocapsa rotundata*) (Strom & Morello, 1998). Cryptophytes, however, are the preferred prey type, based on food vacuole fluorescence in cells offered prey mixtures (Figure S6) and on feeding behavior in prey mixtures (Strom et al., 2020; Strom & Loukos, 1998); they are the only prey type that support sustained *O. lohmannii* growth in culture as monospecific diets.

Feeding on cryptophyte prey is often by myzocytosis (Figure S6). Small-scale flow structures created by the anteriorly located transverse flagellum bring prey to the anterior part of the cell where the peduncle is located (personal observation; see also Nielsen & Kjørboe, 2015). The longitudinal flagellum may also be involved in prey capture, as it has been observed in contact with cryptophyte prey cells (Figure S6). Cells appear to attach to prey at the flattened episome, similar to descriptions of *Amphidinium poecilochroum*

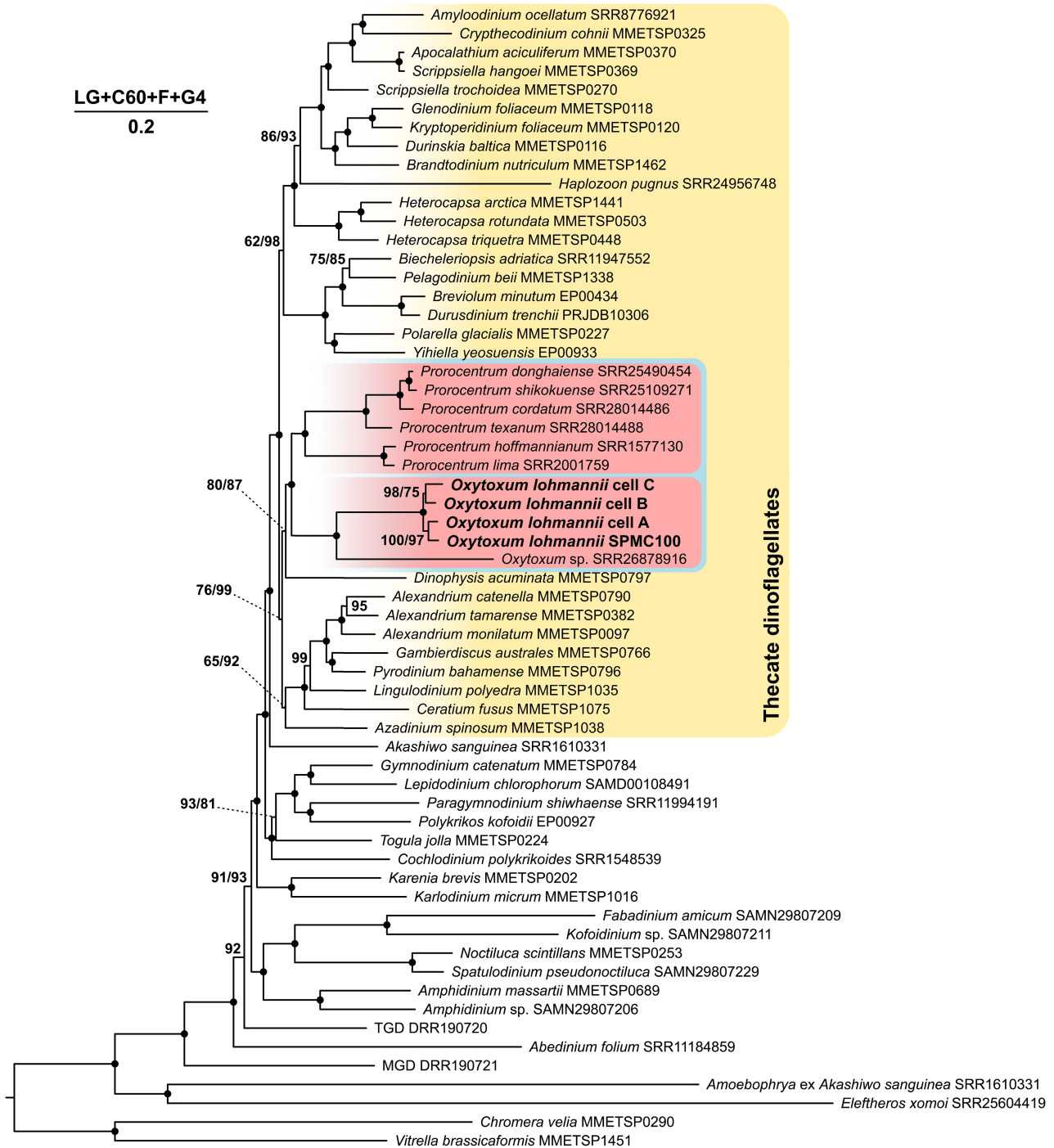


**FIGURE 3** Maximum likelihood (ML) phylogeny of dinoflagellates, including *Oxytoxum lohmannii* and close relatives. Phylogeny is based on 242 protein orthologs, each found in  $\geq 60\%$  of analyzed taxa. Node values depict bootstrap support of the first and second ML analyses, respectively; black dots represent node values of 100/100 and nodes with one number indicate the same support value in both trees. The scale bar provides reference for the estimated number of amino acid substitutions per site, and includes the model used to make the first ML tree, depicted in this figure.

(Larsen, 1988). Epifluorescence revealed prey organelles such as plastids being deformed during passage through the narrow peduncle (Figure S6; see also Strom et al., 2018). Following prey contact, swimming stopped and the prey shrank in size over 20–40s as cytoplasm contents were transferred through the peduncle to the

dinoflagellate. *O. lohmannii* cells starved for more than 1–2 days do not respond quickly to prey additions and only begin feeding hours or days after prey is reintroduced, suggesting that the cells enter a metabolic resting state after a period of time without food (data not shown).

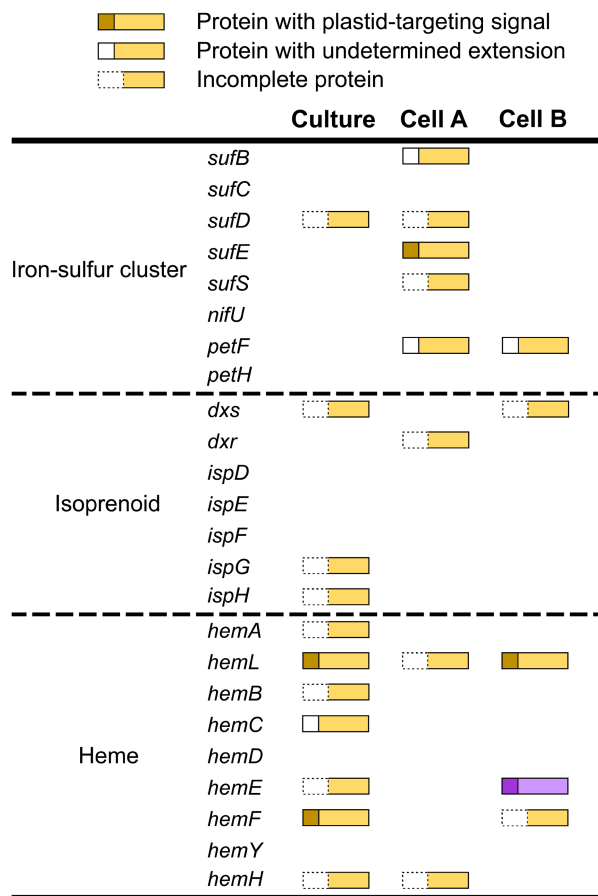


**FIGURE 4** Iron–sulfur cluster, isoprenoid, and heme biosynthesis pathway enzymes found in *Oxytoxum lohmannii* (SPMC100). The N-terminal state of each recovered transcript is depicted as being either a plastid-targeting signal, an undetermined extension (lacking characteristics of a plastid-targeting signal), or incomplete. Yellow transcripts are peridinin plastid derived, while purple indicates apparent haptophyte origin based on single gene phylogenetic analysis (see Data S1 for sequences; single gene trees available at <https://doi.org/10.5061/dryad.9zw3r22pp>).

## DISCUSSION

### Phylogenomic analysis

In contrast to a recent analysis using rRNA genes showing *O. lohmannii* nested within the *Prorocentrum* clade (Gottschling et al., 2024), our more robust multigene phylogenomic analysis places *O. lohmannii* as a sister group to *Prorocentrum*. Due to limited availability of high coverage molecular data for dinoflagellates, fewer taxa are represented in our multigene phylogeny compared with the previous phylogeny of rRNA genes. However, by including all *Prorocentrum* taxa for which transcriptomes are available, we show that this genus is likely monophyletic, with *O. lohmannii* branching outside of the group. This topology suggests that photosynthesis was lost in the ancestor of *O. lohmannii* at some point after it diverged from *Prorocentrum*. Whether

*Oxytoxum* is part of a monophyletic group containing other heterotrophic proro-centrales (*Corythodinium* spp., *Planodinium striatum*) as shown in Gottschling et al. (2024), and how close photosynthetic lineages besides *Prorocentrum* relate to this group remains to be seen once transcriptomic data becomes available for relevant taxa.

### Evidence for a reduced plastid and rhodopsin-based photoactivity

Loss of photosynthesis has occurred multiple times in the evolutionary history of dinoflagellates (Saldarriaga et al., 2001). *Oxytoxum* exemplifies this, as an obligate heterotroph with phylogenetic affinity to photosynthetic taxa. While loss of photosynthesis is common in dinoflagellates and other myzozoans, retention of a reduced plastid organelle is also common, as plastidial biosynthetic pathways for some essential functions have come to replace those of the host (Cooney et al., 2024; Hehenberger et al., 2014; Janouškovec et al., 2017; Mathur et al., 2019). These genes have since moved to the host nucleus, and transcripts have gained N-terminal targeting sequences to guide proteins back to the organelle where they serve their function (Hehenberger et al., 2014).

The plastidial pathways for heme, isoprenoid, and iron–sulfur cluster assembly have been found in most nonphotosynthetic dinoflagellates and myzozoans studied to date (Cooney et al., 2024; Hehenberger et al., 2014; Janouškovec et al., 2017; Mathur et al., 2019). In *O. lohmannii*, the presence of a reduced plastid organelle seems likely, as transcripts for most of these canonical nonphotosynthetic plastid pathways were recovered. Although most transcripts were degraded at the N-terminus, some were complete with signal peptide extensions, suggesting they are targeted to an extant organelle. Interestingly, the assemblages of biosynthesis transcripts found were mostly nonoverlapping between samples. Genes that lacked transcriptional representation were likely not captured due to low expression (as opposed to being absent from the genome), as evidenced by the scant number of contigs for enzymes that were retrieved. In contrast, proteorhodopsin was represented in each transcriptome by several contigs, including in the lowest-coverage sample cell C, which lacked transcripts for plastid biosynthesis enzymes altogether. Furthermore, transcripts of genes making up the same pathway were enriched in the culture (heme) and cell A (iron–sulfur clusters) transcriptomes, suggesting that these functions were being differentially expressed at the time of sampling. Gene homologs found in multiple samples were nearly identical, with the exception of *hemE*, where the homolog from cultured *O. lohmannii* was of peridinin plastid origin, but the homolog recovered from cell B appears to have been acquired horizontally from haptophytes.



These homologs likely coexist in the *O. lohmannii* genome, as this has been seen in other dinoflagellates (Hehenberger et al., 2014, 2019) and myzozoans (Koreny et al., 2011).

The proton pump proteorhodopsin has been described in several dinoflagellates to date, likely acquired through horizontal transfer from bacteria (Béjà et al., 2000; Shi et al., 2015; Slamovits et al., 2011). While its function in eukaryotes is still unclear, there is some evidence to suggest this light-activated pump provides a phototrophic mechanism when feeding or photosynthesis is limited (Guo et al., 2014; Shi et al., 2015). To function in its capacity as a pump, proteorhodopsin requires retinal, a cofactor that binds with the protein and facilitates electron transfer when excited by light (Béjà et al., 2000; Spudich et al., 2000). Retinal is synthesized via the cleavage of carotenoid molecules; however, the specific source molecule and final enzyme catalyst for retinal synthesis varies. All known retinal synthesis enzymes belong to the carotenoid cleavage oxygenase (CCO) family of homologs (Liang et al., 2018). These enzymes are diverse, ubiquitous across the tree of life, and responsible for the formation of many different active carotenoid derivatives; however most of these processes have yet to be described in depth (Liang et al., 2018; Walter & Strack, 2011). Although many heterotrophic eukaryotes are not carotenogenic, the ability to produce CCOs extends to some taxa to digest and repurpose the carotenoids of their prey (Ahrazem et al., 2016). This may be the case in *O. lohmannii* as we found no transcripts of the carotenoid synthesis enzymes *crtB*, *crtI*, and *crtY*, but did recover homologs of three distinct CCOs. The synthesis of retinal by any of these CCOs cannot be confirmed; however, the clear expression of proteorhodopsin in all *O. lohmannii* sampled suggests that this taxon requires retinal, and likely gets it through its diet.

## Growth, chemosensing, and feeding behavior

*Oxytoxum lohmannii* shows low-to-moderate maximum population growth rates, at the low end of the range reported for heterotrophic dinoflagellates (Hansen, 1992; Jeong et al., 2010). While capable of consuming and growing on a variety of prey, *O. lohmannii* appears to be a 'cryptophyte specialist', feeding preferentially on *Pyrenomonas salina* in mixtures with the prymnesiophyte *Isochrysis galbana* (Strom & Loukos, 1998); on *Rhodomonas* sp. in mixtures with the raphidophyte *Heterosigma akashiwo* (Clough & Strom, 2005); and on *Rhodomonas* sp. in mixtures with the haptophyte *Emiliania huxleyi* (Strom et al., 2020).

Relative to other heterotrophic protists, *O. lohmannii* showed high sensitivity to chemical cues, with feeding on a range of algal prey reduced by low  $\mu\text{M}$  concentrations of dimethylsulfoniopropionate (DMSP) and glycine

betaine (Strom, Wolfe, Slajer, et al., 2003). These amino acid derivatives occur at high intracellular concentrations in many phytoplankton, acting as compatible osmolytes and, perhaps, antioxidants (Bullock et al., 2017). Thus, these molecules would be readily released from stressed (i.e., membrane-compromised) or wounded cells. *O. lohmannii* was also the most sensitive of 6 tested protist predators to the DMSP lyase activity level of its prey (as represented by a range of *E. huxleyi* isolates; Strom, Wolfe, Holmes, et al., 2003); while low lyase strains were readily ingested and supported *O. lohmannii* growth, high lyase strains were essentially not eaten (Strom et al., 2018; Strom, Wolfe, Holmes, et al., 2003). Since the lyase products DMS and acrylate were not inhibitory, the lack of feeding was attributed to localized high concentrations of precursor DMSP, and/or to distinctive prey cell surface characteristics. Overall, the combination of high discrimination among prey types in a mixture and high sensitivity to algal-derived dissolved (and perhaps cell surface) cues suggests a substantial role for 'information gathering' in *O. lohmannii*'s feeding behavior.

A fascinating aspect of *O. lohmannii* autecology is the presence of multiple, apparently prey-specific feeding modes. The dinoflagellate can use myzocytosis to feed on cryptophyte prey (although it has also been observed using conventional phagocytosis on *Rhodomonas salina* at the site of the peduncle: Gottschling et al., 2024). This strategy, which employs the peduncle situated on the episome anterior, originating from a flange-like structure (Figure 1, Figure S6D), might be in part an adaptation for penetrating the distinctive glycoprotein scales that surround cryptophyte cells (Brett et al., 1994). We observed prominent peduncles in numerous SEM images of both starved and feeding *O. lohmannii*. However, the lag in feeding following prolonged starvation raises the possibility that the peduncle or other feeding apparatus needs to be activated following starvation. We also observed cryptophyte prey successfully escape capture after contact. Many pallium- or peduncle-feeding taxa employ capture filaments to tether to large prey (Hansen & Calado, 1999). *O. lohmannii* has an unusually large number of trichocysts, many concentrated in the episome where prey contact occurs, but their role in prey capture is still uncertain. We observed discharged trichocysts emerging from the episome in numerous epifluorescence micrographs (Figure S6A,B), but these were likely artifacts of gluteraldehyde preservation. In SEM preparations fixed with osmium, we observed trichocysts less frequently, but sometimes these were touching prey cells, raising the possibility that episome trichocysts may be used as capture filaments.

*Oxytoxum lohmannii* uses phagocytosis at the site of the peduncle (Gottschling et al., 2024) to ingest non-cryptophyte phytoflagellates, including the haptophyte

*Emiliana huxleyi* (smaller than most cryptophytes; attachment of a cell shown in Figure S6E) and the photosynthetic dinoflagellate *Heterocapsa rotundata* (larger than most cryptophytes). More-or-less intact cells of these species can be seen inside *O. lohmannii* food vacuoles, with single vacuoles often containing multiple discrete cells of *E. huxleyi*. This contrasts with the generalized orange fluorescence that results when partially digested cryptophytes make their way into the vacuole through the peduncle (Figure S6D, Strom et al., 2018). Phagocytosis by thecate dinoflagellates, whether photosynthetic or heterotrophic, is well known (e.g., Jeong et al., 2010). The use of multiple feeding modes by a single dinoflagellate species appears less common. The mixotrophic, toxin-producing genus *Karlodinium* is one of the few known examples. Depending on the species, *Karlodinium* feeds using a peduncle or modified peduncle in addition to phagocytosis; a capture filament has also been observed in some cases (Yang et al., 2021).

## CONCLUSIONS

Dinoflagellates are a complex assemblage of protists offering insights into trophic nuance, unique cell biology, and unexpected evolutionary history. The raptorial heterotroph *Oxytoxum lohmannii* embodies this reputation with its multifaceted feeding behavior, bacterial photobiology, and recent photosynthetic ancestry. The possession of proteorhodopsin by this species can also provide insight into this alternate form of photoactivity in eukaryotes. Because this species is readily maintained in culture, it is a strong candidate for the study of heterotrophic dinoflagellate cell biology, food preference, and chemical ecology. Further microscopy is needed to understand the unique mucocysts and peduncle-feeding mechanism of *O. lohmannii*. Ultimately, understanding chemosensing and feeding behavior will require the elucidation of this dinoflagellate's electrophysiology and signal transduction network, something only attempted in larger alveolates (Echevarria et al., 2016).

## ACKNOWLEDGMENTS

We thank the WWU biology department for the gift of the critical-point dryer, and Richard Demaree for the use of, and help with, CSU Chico electron microscope facilities. We also thank Dr. Sunita Sinha at the Sequencing and Bioinformatics Consortium (UBC) with her extensive assistance with sequencing optimization. This research was supported by National Science Foundation grant OCE-9730952, the Gordon and Betty Moore Foundation (<https://doi.org/10.37807/GBMF9201>; PJK), and the Natural Sciences and Engineering Research Council of Canada grants NSERC 2019-03986 (BSL) and NSERC 2019-03994 (PJK).

## ORCID

Elizabeth C. Cooney  <https://orcid.org/0000-0001-7435-7609>  
 Brian S. Leander  <https://orcid.org/0000-0003-0798-0470>

## REFERENCES

- Ahrazem, O., Gómez-Gómez, L., Rodrigo, M.J., Avalos, J. & Limón, M.C. (2016) Carotenoid cleavage oxygenases from microbes and photosynthetic organisms: features and functions. *International Journal of Molecular Sciences*, 17, 1–38.
- Altschul, S.F., Gish, W., Miller, W., Myers, E.W. & Lipman, D.J. (1990) Basic local alignment search tool. *Journal of Molecular Biology*, 215, 403–410. Available from: [https://doi.org/10.1016/S0022-2836\(05\)80360-2](https://doi.org/10.1016/S0022-2836(05)80360-2)
- Bankevich, A., Nurk, S., Antipov, D., Gurevich, A.A., Dvorkin, M., Kulikov, A.S. et al. (2012) SPAdes: a new genome assembly algorithm and its applications to single-cell sequencing. *Journal of Computational Biology*, 19, 455–477.
- Béjà, O., Aravind, L., Koonin, E.V., Suzuki, M.T., Hadd, A., Nguyen, L.P. et al. (2000) Bacterial rhodopsin: evidence for a new type of phototrophy in the sea. *Science*, 289, 1902–1906. Available from: <https://doi.org/10.1126/science.289.5486.1902>
- Blum, M., Chang, H., Chuguransky, S., Grego, T., Kandasamy, S., Mitchell, A. et al. (2021) The InterPro protein families and domains database: 20 years on. *Nucleic Acids Research*, 49, 344–354.
- Brett, S.J., Perasso, L. & Wetherbee, R. (1994) Structure and development of the cryptomonad periplast: a review. *Protoplasma*, 181, 106–122.
- Bullock, H.A., Luo, H. & Whitman, W.B. (2017) Evolution of dimethylsulfoniopropionate metabolism in marine phytoplankton and bacteria. *Frontiers in Microbiology*, 8, 1–17.
- Burki, F., Kaplan, M., Tikhonenkov, D.V., Zlatogursky, V., Minh, B.Q., Radaykina, L.V. et al. (2016) Untangling the early diversification of eukaryotes: a phylogenomic study of the evolutionary origins of Centrohelida, Haptophyta and Cryptista. *Proceedings of the Royal Society B: Biological Sciences*, 283, 1–10.
- Capella-Gutiérrez, S., Silla-Martínez, J.M. & Gabaldón, T. (2009) trimAl: A tool for automated alignment trimming in large-scale phylogenetic analyses. *Bioinformatics*, 25, 1972–1973.
- Chu, F.L.E., Lund, E.D., Littreal, P.R., Ruck, K.E. & Harvey, E. (2009) Species-specific differences in long-chain n-3 essential fatty acid, sterol, and steroidal ketone production in six heterotrophic protist species. *Aquatic Biology*, 6, 159–172.
- Clough, J. & Strom, S. (2005) Effects of *Heterosigma akashiwo* (Raphidophyceae) on protist grazers: laboratory experiments with ciliates and heterotrophic dinoflagellates. *Aquatic Microbial Ecology*, 39, 121–134.
- Cooney, E.C., Holt, C.C., Hehenberger, E., Adams, J.A., Leander, B.S. & Keeling, P.J. (2024) Investigation of heterotrophs reveals new insights in dinoflagellate evolution. *Molecular Phylogenetics and Evolution*, 196, 108086. Available from: <https://doi.org/10.1016/j.ympev.2024.108086>
- Echevarria, M.L., Wolfe, G.V. & Taylor, A.R. (2016) Feast or flee: bioelectrical regulation of feeding and predator evasion behaviors in the planktonic alveolate *Favella* sp. (Spirotruchia). *The Journal of Experimental Biology*, 219, 445–456.
- Fenchel, T. (2001) How dinoflagellates swim. *Protist*, 152, 329–338.
- Fitt, W.K. (1985) Chemosensory responses of the symbiotic dinoflagellate *Symbiodinium microadriaticum* (Dinophyceae). *Journal of Phycology*, 21, 62–67.
- Gaines, G. & Elbrächter, M. (1987) Heterotrophic nutrition. In: Taylor, F.J.R. (Ed.) *The biology of dinoflagellates*, Vol. 21. Oxford: Blackwell, pp. 224–268.
- Gottschling, M., Wietkamp, S., Bantle, A. & Tillmann, U. (2024) Oxytoxaceae are prorocentralean rather than

- peridinialean dinophytes and taxonomic clarification of heterotrophic *Oxytoxum lohmannii* by epitypification. *Scientific Reports*, 14, 6689. Available from: <https://doi.org/10.1038/s41598-024-56848-y>
- Guo, Z., Zhang, H. & Lin, S. (2014) Light-promoted rhodopsin expression and starvation survival in the marine dinoflagellate *Oxyrrhis marina*. *PLoS One*, 9, 1–23.
- Haas, B.J., Papanicolaou, A., Yassour, M., Grabherr, M., Blood, P.D., Bowden, J. et al. (2013) De novo transcript sequence reconstruction from RNA-seq using the trinity platform for reference generation and analysis. *Nature Protocols*, 8, 1494–1512.
- Hansen, P.J. (1992) Prey size selection, feeding rates and growth dynamics of heterotrophic dinoflagellates with special emphasis on *Gyrodinium spirale*. *Marine Biology*, 114, 327–334.
- Hansen, P.J. & Calado, A.J. (1999) Phagotrophic mechanisms and prey selection in free-living dinoflagellates. *The Journal of Eukaryotic Microbiology*, 46, 382–389.
- Hauser, D.C.R., Levandowsky, M. & Glassgold, J.M. (1975a) Ultrasensitive chemosensory responses by a protozoan to epinephrine and other neurochemicals. *Science*, 190, 285–286.
- Hauser, D.C.R., Levandowsky, M., Hutner, S.H., Chunosoff, L. & Hollwitz, J.S. (1975b) Chemosensory responses by the heterotrophic marine dinoflagellate *Cryptecodinium cohnii*. *Microbial Ecology*, 1, 246–254.
- Hehenberger, E., Gast, R.J. & Keeling, P.J. (2019) A kleptoplastidic dinoflagellate and the tipping point between transient and fully integrated plastid endosymbiosis. *Proceedings of the National Academy of Sciences of the United States of America*, 116, 17934–17942.
- Hehenberger, E., Imanian, B., Burki, F. & Keeling, P.J. (2014) Evidence for the retention of two evolutionary distinct plastids in dinoflagellates with diatom endosymbionts. *Genome Biology and Evolution*, 6, 2321–2334.
- Hoang, D.T., Chernomor, O., Von Haeseler, A., Minh, B.Q. & Vinh, L.S. (2018) UFBoot2: improving the ultrafast bootstrap approximation. *Molecular Biology and Evolution*, 35, 518–522.
- Jacobson, D.M. & Anderson, D.M. (1986) Thecate heterotrophic dinoflagellates: feeding behavior and mechanisms. *Journal of Phycology*, 22, 249–258.
- Jacobson, D.M. & Anderson, D.M. (1992) Ultrastructure of the feeding apparatus and myonemal system of the heterotrophic dinoflagellate *Protoperidinium spinolosum*. *Journal of Phycology*, 28, 69–82.
- Janouškovec, J., Gavelis, G.S., Burki, F., Dinh, D., Bachvaroff, T.R., Gornik, S.G. et al. (2017) Major transitions in dinoflagellate evolution unveiled by phylotranscriptomics. *Proceedings of the National Academy of Sciences of the United States of America*, 114, E171–E180. Available from: <https://doi.org/10.1073/pnas.1614842114>
- Jeong, H.J., Shim, J.H., Lee, C.W., Kim, J.S. & Koh, S.M. (1999) Growth and grazing rates of the marine planktonic ciliate *Strombidinopsis* sp. on red-tide and toxic dinoflagellates. *The Journal of Eukaryotic Microbiology*, 46, 69–76.
- Jeong, H.J., Yoo, Y., Du, K.J.S., Seong, K.A., Kang, N.S. & Kim, T.H. (2010) Growth, feeding and ecological roles of the mixotrophic and heterotrophic dinoflagellates in marine planktonic food webs. *Ocean Science Journal*, 45, 65–91. Available from: <https://doi.org/10.1007/s12601-010-0007-2>
- Kalyaanamoorthy, S., Minh, B.Q., Wong, T.K.F., Von Haeseler, A. & Jermiin, L.S. (2017) ModelFinder: fast model selection for accurate phylogenetic estimates. *Nature Methods*, 14, 587–589.
- Katoh, K. & Standley, D.M. (2013) MAFFT multiple sequence alignment software version 7: improvements in performance and usability. *Molecular Biology and Evolution*, 30, 772–780.
- Keeling, P.J. (2013) The number, speed, and impact of plastid endosymbioses in eukaryotic evolution. *Annual Review of Plant Biology*, 64, 583–607.
- Keeling, P.J. & del Campo, J. (2017) Marine protists are not just big bacteria. *Current Biology*, 27, R541–R549. Available from: <https://doi.org/10.1016/j.cub.2017.03.075>
- Kofoed, C.A. & Swezy, O. (1921) *The free-living unarmored Dinoflagellata*. Berkeley, CA: University of California Press.
- Kolisko, M., Boscaro, V., Burki, F., Lynn, D.H. & Keeling, P.J. (2014) Single-cell transcriptomics for microbial eukaryotes. *Current Biology*, 24, R1081–R1082. Available from: <https://doi.org/10.1016/j.cub.2014.10.026>
- Koreny, L., Sobotka, R., Janouškovec, J., Keeling, P.J. & Obornik, M. (2011) Tetrapyrrole synthesis of photosynthetic chromerids is likely homologous to the unusual pathway of apicomplexan parasites. *Plant Cell*, 23, 3454–3462.
- Larsen, J. (1988) An ultrastructural study of *Amphidinium poecilochroum* (Dinophyceae), a phagotrophic dinoflagellate feeding on small species of cryptophytes. *Phycologia*, 27, 366–377.
- Levandowsky, M. & Hauser, D.C.R. (1975) Chemosensory responses of swimming algae and protozoa. *International Review of Cytology*, 53, 175–210.
- Liang, M.-H., Zhu, J. & Jiang, J.-G. (2018) Carotenoids biosynthesis and cleavage related genes from bacteria to plants. *Critical Reviews in Food Science and Nutrition*, 58, 2314–2333. Available from: <https://doi.org/10.1080/10408398.2017.1322552>
- Man, D., Wang, W., Sabehi, G., Aravind, L., Post, A.F., Massana, R. et al. (2003) Diversification and spectral tuning in marine proteorhodopsins. *The EMBO Journal*, 22, 1725–1731.
- Martin, M. (2011) Cutadapt removes adapter sequences from high-throughput sequencing reads. *EMBnet Journal*, 17, 10–12.
- Mathur, V., Kolisko, M., Hehenberger, E., Irwin, N.A.T., Leander, B.S., Kristmundsson, Á. et al. (2019) Multiple independent origins of apicomplexan-like parasites. *Current Biology*, 29, 2936–2941.
- Nielsen, H., Engelbrecht, J., Brunak, S. & von Heijne, G. (1997) Identification of prokaryotic and eukaryotic signal peptides and prediction of their cleavage sites. *Protein Engineering*, 10, 1–6.
- Nielsen, L.T. & Kjørboe, T. (2015) Feeding currents facilitate a mixotrophic way of life. *The ISME Journal*, 9, 2117–2127.
- Picelli, S., Faridani, O.R., Björklund, Å.K., Winberg, G., Sagasser, S. & Sandberg, R. (2014) Full-length RNA-seq from single cells using smart-seq2. *Nature Protocols*, 9, 171–181.
- Poux, S., Arighi, C.N., Magrane, M., Bateman, A., Wei, C.H., Lu, Z. et al. (2017) On expert curation and scalability: UniProtKB/swiss-Prot as a case study. *Bioinformatics*, 33, 3454–3460.
- Quang, L.S., Gascuel, O. & Lartillot, N. (2008) Empirical profile mixture models for phylogenetic reconstruction. *Bioinformatics*, 24, 2317–2323.
- Roure, B., Rodriguez-Ezpeleta, N. & Philippe, H. (2007) SCaFoS: a tool for selection, concatenation and fusion of sequences for phylogenomics. *BMC Evolutionary Biology*, 7, 1–12.
- Saldarriaga, J.F., Taylor, F.J.R., Keeling, P.J. & Cavalier-Smith, T. (2001) Dinoflagellate nuclear SSU rRNA phylogeny suggests multiple plastid losses and replacements. *Journal of Molecular Evolution*, 53, 204–213.
- Sarai, C., Tanifuji, G., Nakayama, T., Kamikawa, R., Takahashi, K., Yazaki, E. et al. (2020) Dinoflagellates with relic endosymbiont nuclei as models for elucidating organellogenesis. *Proceedings of the National Academy of Sciences of the United States of America*, 117, 5364–5375.
- Schnepf, E. & Drebes, G. (1986) Chemotaxis and appetite of *Paulsenella* sp. (Dinophyta), an ectoparasite of the marine diatom *Streptotheca thamesis* Shrubsole. *Planta*, 167, 337–343.
- Schnepf, E. & Elbrächter, M. (1992) Nutritional strategies in dinoflagellates: a review with emphasis on cell biological aspects. *European Journal of Protistology*, 28, 3–24.
- Sherr, E.B. & Sherr, B.F. (1994) Bacterivory and herbivory: key roles of phagotrophic protists in pelagic food webs. *Microbial Ecology*, 28, 223–235.
- Shi, X., Li, L., Guo, C., Lin, X., Li, M. & Lin, S. (2015) Rhodopsin gene expression regulated by the light dark cycle, light spectrum and light intensity in the dinoflagellate *Prorocentrum*. *Frontiers in Microbiology*, 6, 1–11.



- Slamovits, C.H., Okamoto, N., Burri, L., James, E.R. & Keeling, P.J. (2011) A bacterial proteorhodopsin proton pump in marine eukaryotes. *Nature Communications*, 2, 183.
- Sonnhammer, E.L.L., von Heijne, G. & Krogh, A. (1998) A hidden Markov model for predicting transmembrane helices in protein sequences. *Proceedings. International Conference on Intelligent Systems for Molecular Biology*, 6, 175–182.
- Spero, H.J. (1985) Chemosensory capabilities in the phagotrophic dinoflagellate *Gymnodinium fungiforme*. *Journal of Phycology*, 21, 181–184.
- Spudich, J.L., Yang, C.S., Jung, K.H. & Spudich, E.N. (2000) Retinylidene proteins: structures and functions from archaea to humans. *Annual Review of Cell and Developmental Biology*, 16, 365–392. Available from: <https://doi.org/10.1146/annurev.cellbio.16.1.365>
- Stamatakis, A. (2006) RAxML-VI-HPC: maximum likelihood-based phylogenetic analyses with thousands of taxa and mixed models. *Bioinformatics*, 22, 2688–2690.
- Stoecker, D.K. (1999) Mixotrophy among dinoflagellates. *The Journal of Eukaryotic Microbiology*, 46, 397–401.
- Strom, S., Wolfe, G., Holmes, J., Stecher, H., Shimeneck, C., Lambert, S. et al. (2003a) Chemical defense in the microplankton I: feeding and growth rates of heterotrophic protists on the DMS-producing phytoplankton *Emiliana huxleyi*. *Limnology and Oceanography*, 48, 217–229.
- Strom, S., Wolfe, G., Slajer, A., Lambert, S. & Clough, J. (2003b) Chemical defense in the microplankton II: inhibition of protist feeding by B-dimethylsulfoniopropionate (DMSP). *Limnology and Oceanography*, 48, 230–237.
- Strom, S.L., Barberi, O., Mazur, C., Bright, K.J. & Fredrickson, K.A. (2020) High light stress reduces dinoflagellate predation on phytoplankton through both direct and indirect responses. *Aquatic Microbial Ecology*, 84, 43–57.
- Strom, S.L., Bright, K.J., Fredrickson, K.A. & Cooney, E.C. (2018) Phytoplankton defenses: do *Emiliana huxleyi* coccoliths protect against microzooplankton predators? *Limnology and Oceanography*, 63, 617–627.
- Strom, S.L. & Loukos, H. (1998) Selective feeding by protozoa: model and experimental behaviors and their consequences for population stability. *Journal of Plankton Research*, 20, 831–846.
- Strom, S.L. & Morello, T.A. (1998) Comparative growth rates and yields of ciliates and heterotrophic dinoflagellates. *Journal of Plankton Research*, 20, 571–584.
- Taylor, F.J.R., Hoppenrath, M. & Saldarriaga, J.F. (2008) Dinoflagellate diversity and distribution. *Biodiversity and Conservation*, 17, 407–418.
- Walter, M.H. & Strack, D. (2011) Carotenoids and their cleavage products: biosynthesis and functions. *Natural Product Reports*, 28, 663–692.
- Wang, H.-C., Minh, B.Q., Susko, E. & Roger, A.J. (2018) Modeling site heterogeneity with posterior mean site frequency profiles accelerates accurate phylogenomic estimation. *Systematic Biology*, 67, 216–235.
- Wilcox, L.W. & Wedemayer, G.J. (1991) Phagotrophy in the freshwater, photosynthetic dinoflagellate *Amphidinium cryophilum*. *Journal of Phycology*, 27, 600–609.
- Yang, H., Hu, Z. & Tang, Y.Z. (2021) Plasticity and multiplicity of trophic modes in the dinoflagellate *Karlodinium* and their pertinence to population maintenance and bloom dynamics. *Journal of Marine Science and Engineering*, 9, 1–21.

## SUPPORTING INFORMATION

Additional supporting information can be found online in the Supporting Information section at the end of this article.

**How to cite this article:** Cooney, E.C., Jacobson, D.M., Wolfe, G.V., Bright, K.J., Saldarriaga, J.F., Keeling, P.J. et al. (2024) Morphology, behavior, and phylogenomics of *Oxytoxum lohmannii*, Dinoflagellata. *Journal of Eukaryotic Microbiology*, 00, e13050. Available from: <https://doi.org/10.1111/jeu.13050>